Proceedings 10th NUMGE 2023
10th European Conference on Numerical Methods in Geotechnical Engineering
Zdravkovic L, Kontoe S, Taborda DMG, Tsiampousi A (eds)

https://doi.org/10.53243/NUMGE2023-428

Numerical analysis of the impact of driving imperfection on the water pressure resistance of HZ®-M walls

R. Matos[1], C. Prüm[1], A. El Kasimi[2], O. Hechler[2]

[1]*ArcelorMittal Global R&D, Esch-sur-Alzette, Luxembourg*
[2]*ArcelorMittal Sheet Piling, Esch-sur-Alzette, Luxembourg*

ABSTRACT: The HZ®-M wall system is a retaining wall solution commonly applied in marine structures (ports and waterways) and structures subjected to high water pressure loading (dry docks and cofferdams). This system is a combined wall system composed of special H-shaped piles (king piles - main bending resistance element) and intermediary sheet piles (secondary piles normally considered as filling elements to transfer loads to the king piles). Current design water pressure resistances for systems without driving imperfections in normal (compression) direction are available based on previous research. This paper presents a comprehensive study on a numerical modelling technique to properly estimate the water pressure resistance of HZ®-M walls subjected to water pressure, with or without driving imperfections, following the recommendations of the new generation of Eurocodes on design based numerical analysis. The strain-based and stability-based approaches are addressed. The validation and accuracy of the numerical results are further presented to demonstrate the reliability of the technique.

Keywords: HZ®-M wall; sheet piles; water pressure; infill sheet resistance; driving imperfections

1 INTRODUCTION

Steel sheet pile walls are structures driven in the ground to retain ground and/or water. They are a very well-established solution with a wide range of capacity from low to medium bending resistance in the case of corrugated sheet piles, e.g. AZ sheet piles (Figure 1) and high resistance in the case of combined walls. A combined wall is an embedded retaining wall composed of primary and secondary elements. For HZ®-M walls, the primary elements are normally H piles, spaced uniformly along the length of the wall. The secondary elements are generally steel sheet piles installed in the spaces between the primary elements and connected to them by interlocks (CEN, 2022).

In this solution it is generally considered that the H piles (king piles) are the elements responsible for the global bending resistance of the wall while the infill sheet piles are responsible to retain the soil pressures behind the wall and assure e.g., water tightness. They transfer the retained loads to the king piles via connectors.

The sheet piles most commonly applied in the HZ®-M walls are the AZ geometry (Figure 1) and assembled in pairs of two (double piles). Depending on the external loading, the king piles can be installed as single or double (box) (Figure 2).

This HZ®-M solution is commonly used also for applications where a water pressure is a very relevant load case, such as dry docks and cofferdams.

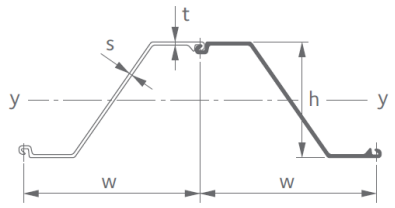

Figure 1. AZ sheet pile geometry (ArcelorMittal Sheet Piling, 2020)

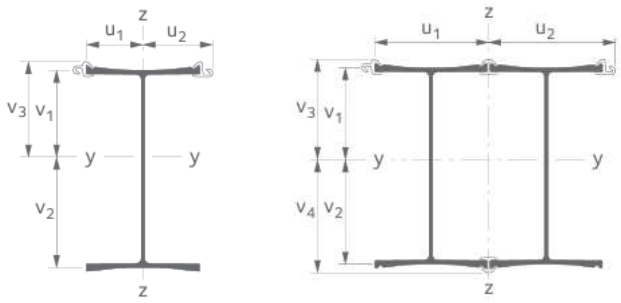

a. *single* b. *double*

Figure 2. HZ-M king piles geometry (ArcelorMittal Sheet Piling, 2020)

The infill sheet piles under water pressure can work in compression (Figure 3.a) or in tension (Figure 3.b). This study will focus on the effect of water pressure resistance in systems where infill sheet piles are working in compression. This is the most common configuration as it allows the creation of a straight wall front. However, when infill sheet piles are working in tension, a

higher bending and water pressure resistance is attained due to the mobilization of the membrane effect.

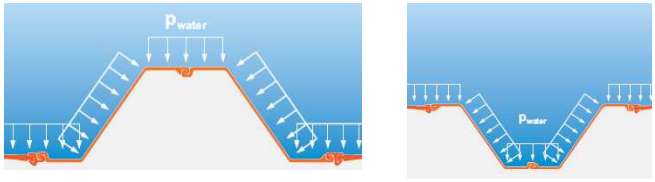

a. *infill sheet in compression*

b. *infill sheets in tension*

Figure 3. HZ®-M wall under water pressure (ArcelorMittal Sheet Piling, 2020)

For the installation of combined walls, first the king piles are driven into the ground, guided by a template, and subsequently the infill sheets are driven between the king piles. The geometry of the infill sheets and interlocks thereby provide flexibility to account for driving imperfection of the king piles within given limits. The magnitude of the acceptable driving tolerances is requested for design (CEN, 2007) and should be agreed for each project (CEN, 2022).

The ultimate position of the bearing piles defines the final wall geometry, which determines the stress state and thus also the load-bearing behaviour of the elements subjected to water pressure (Chrzanowski et al., 2021).

This paper aims to describe and validate a numerical procedure to properly assess the water pressure resistance of HZ®-M walls accounting for driving imperfections. Even though the main topic of this paper is the analysis of the water pressure resistance of combined walls, this numerical technique is valid also to estimate the pressure resistance of the wall subjected to soft soils that will not generate an arching effect. The water pressure (soft soil) will be modelled using an increasing pressure loading.

The 2D analysis (cross-section analysis) conducted in this study is based in the assumption that the highest pressure in the wall is coincident with the point of highest driving imperfection leading therefore to a safe sided approach of the problem.

2 DESIGN CRITERIA

Simplifying for global design, the inertia of the system can be considered as the sum of the individual inertias of all the elements, as described in Equation (1). The value of the inertia per meter of wall is obtained by dividing the inertia of the system by its width (b_{sys}).

$$I_{sys} = I_{HZ} + I_{AZ} \tag{1}$$

To determine the acting bending moment in each individual element, Equations (2) and (3) must be considered, respectively, for the H pile or infill sheet.

$$M_{HZ} = \left(\frac{I_{HZ}}{I_{sys}} M_{sys}\right) b_{sys} \tag{2}$$

$$M_{AZ} = \left(\frac{I_{AZ}}{I_{sys}} M_{sys}\right) b_{sys} \tag{3}$$

where M_{sys} refers to the total acting bending moment per meter of wall

The stress verification can then be done using the Equations (4-6).

$$\sigma_{HZ} = \frac{M_{sys}}{W_{el,y^*}} \tag{4}$$

$$\sigma_{\frac{RH}{RZ}} = \frac{M_{sys}}{W_{el,y^{**}}} \tag{5}$$

$$\sigma_{AZ} = \left(\frac{I_{AZ}}{I_{sys}} . b_{sys}\right) \times \frac{M_{sys}}{W_{AZ}} \tag{6}$$

In a global safety approach, the safety of the system is ensured if the acting stress is lower than the yield stress of each individual element divided by the safety factor.

If a partial safety approach is to be considered, the semi-probabilistic approach according to the Eurocode series should be applied (CEN, 2002). It is a partial safety factor approach applying safety factors both to the loads as well as to the resistances, before performing the stress verification as described in Equations (4-6).

Even though the assumption of bending moment distribution between king pile and secondary pile are offering some optimisation to the system, it is often neglected. Indeed, to simplify the system, the assumption of soil arching is often made, meaning that the king pile is the main bearing element whereas the secondary piles only fill the gap and thus only transfer water pressure loads to the king pile. Hence, it is necessary to verify their resistance to water pressure and their ability to transfer these loads to the king piles.

EC3-5 (CEN, 2007) offers three possible ways of verification, namely:

- if some specific criteria are met, the verification can be omitted
- experimental testing
- numerical modelling

This study focusses in the design by numerical modelling of the water pressure capacity according to prEN 1993-1-14 (CEN, 2021).

3 NUMERICAL MODEL DESCRIPTION

3.1 Framework

In the new draft prEN 1993-1-14 (CEN, 2021), two criterions (C1 and C2) should be used to evaluate the resistance of one element/structure with finite element modelling, as illustrated in Figure 4. Elements subject

to compression and a risk of buckling will typically follow a curve with a maximum (C1), whereas elements in tension will typically follow an increasing curve for which the failure will be reached at maximum allowable strain (C2). Information on maximum allowable strain for secondary piles can be found in EN 1993-5 (CEN, 2007).

Depending on the stiffness and geometry of the system, either the maximum strain (C2) or the maximum load (stability) (C1) is reached first. Thus, both approaches give different results in terms of maximum load and should be considered.

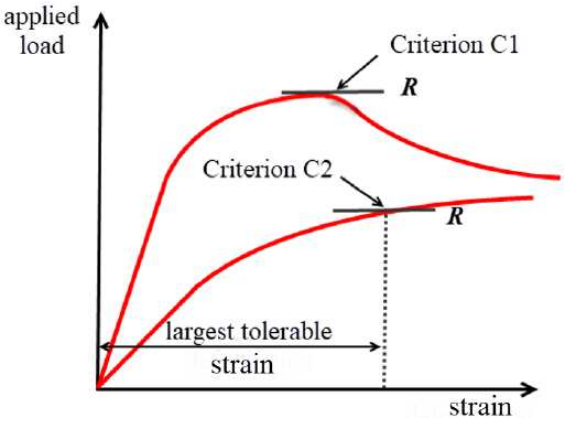

Figure 4. Criterion C1 and C2 for estimation of resistance (prEN 1993-1-14 (CEN, 2021))

3.2 Geometry and material model

The numerical model used in this analysis was developed using the software Abaqus (2017). It is a 2D model with solid elements (continuum solid) and with contact elements between the sheet piles and the HZ, as well as between both sheet piles, as described in Figure 5. Tie constrains were added to simulate the welding between the external connector and the beam.

The model was divided in four distinct parts (2 king piles + connectors and 2 sheet piles) and the elements used in all the parts were CPS4R (4-node bilinear plane stress quadrilateral, reduced integration, hourglass control) with standard configuration. Non-linear geometry was set "on" for all load cases.

It was considered a frictional contact with a coefficient of 0.25 between the different elements and, as boundary conditions, it was considered a fully fixed support in the surfaces of the king piles, as depicted in Figure 5(a). The external pressure (water pressure or soft soil) was applied in the full edge of the sheet piles and in the king pile flanges as illustrated in Figure 5(b).

The mesh was more refined close to the areas of higher stress variation and higher deformation to be expected (flange of the king pile with the connection and interlocks and radius of the sheet piles), as illustrated in Figure 6. The mesh was tried to be as uniform as possible and with a low form factor to assure numerical analysis stability (lower than 4 when possible).

The material model (elasto-plastic with hardening) was defined up to the necking region. After the value of ε_3 the strain increased with no increase in the stress.

The parameters for the material curve were defined according to BSK99 (2003) standard (Figure 7). For this analysis the considered values of f_y and f_u are, respectively, 430MPa and 510Mpa while the values of ε_1, ε_2, ε_3 and ε_{max} are, respectively, 0.00205, 0.01286, 0.03905 and 0.114.

(a) boundary conditions

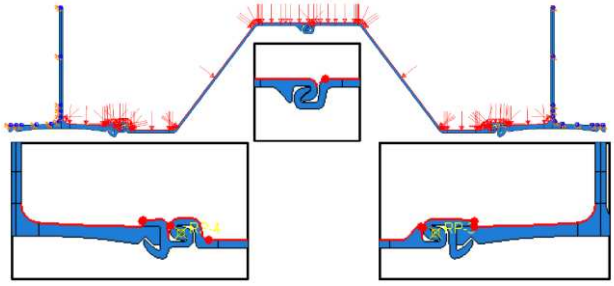

(b) loading conditions

Figure 5. Numerical model general geometry

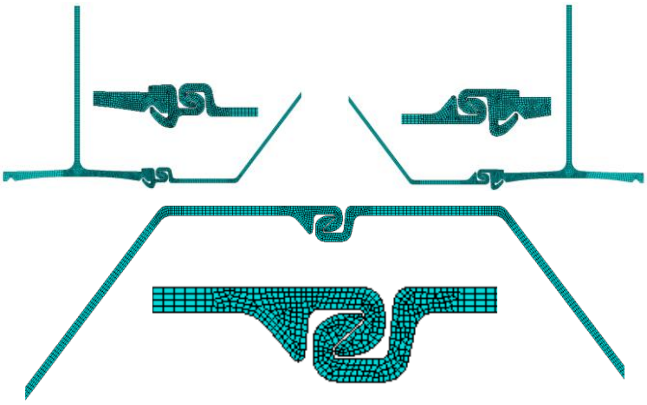

Figure 6. Numerical model mesh

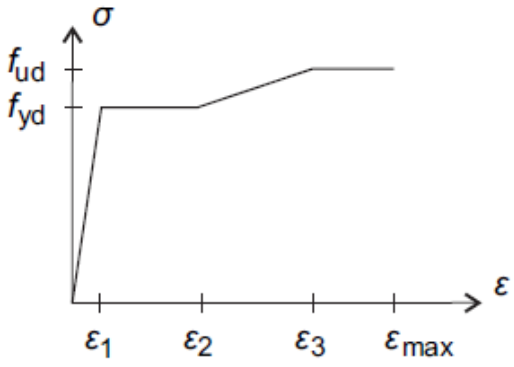

Figure 7. Material model definition (BSK99, 2003)

3.3 Validation

To validate the accuracy of the numerical model procedure, a comparison with experimental results was performed. A set of experimental tests was conducted by Just (2020). The test setup is presented in Figure 8 and the external loading is applied by means of prescribed displacement in two points of the top flange of the sheet pile.

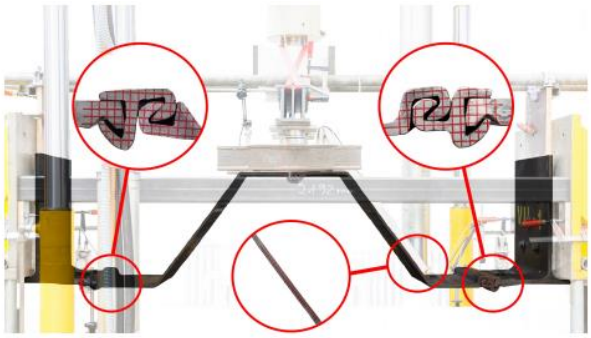

Figure 8. Experimental test setup – initial loading step (Just, 2020)

The load-displacement response of the test specimens with AZ25-800 infill sheet piles from test series VII (Just, 2020) and the performed FE simulations are compared in Figure 9. The washed lines are sourced from the work of Just (2020). The more visible blue, red and grey lines show the result of the performed FE simulation within this investigation. The red line refers to the simulations with material laws with properties according to material tensile tests reported in Just (2020) (including an assumed descending branch), whereas the grey and blue lines represent, respectively, the response for the material EN+BSK unmodified (according to Figure 7) and modified (as in Figure 7 but including also an assumed descending branch), as detailed in Chrzanowski et al. (2021).

From Figure 9, it can be observed that good coherence between test and FE results was obtained. The same ultimate load and overall character of the response were achieved. Therefore, the model has been considered accepted.

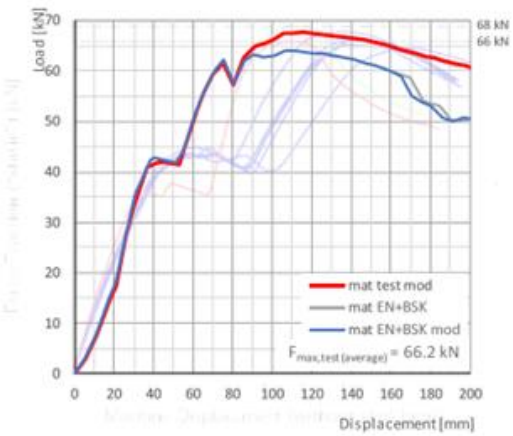

Figure 9. Experimental vs. numerical results

3.4 Accounting for driving imperfections in the numerical analysis

With the aim to analyse the effect of driving imperfections on the system, all possible displacements of HZ®-M king piles were considered (Figure 10): (i) horizontal displacement (stretching/compression of the system), (ii) Out-plane displacement (upward and downward), (iii) rotation around the centres of the HZ®-M king piles (clockwise and counter clockwise).

Any other displacement is composed of several independent displacements shown in Figure 10. E.g., a rotation around the centre of the king pile is in fact a combination of translations and rotation at the interlock.

4 NUMERICAL TECHNIQUES TO MODEL DIFFERENT FAILURE MODES

4.1 Introduction

The numerical procedure for an accurate characterization of the behaviour of HZ®-M walls under water pressure is presented in Section 4.

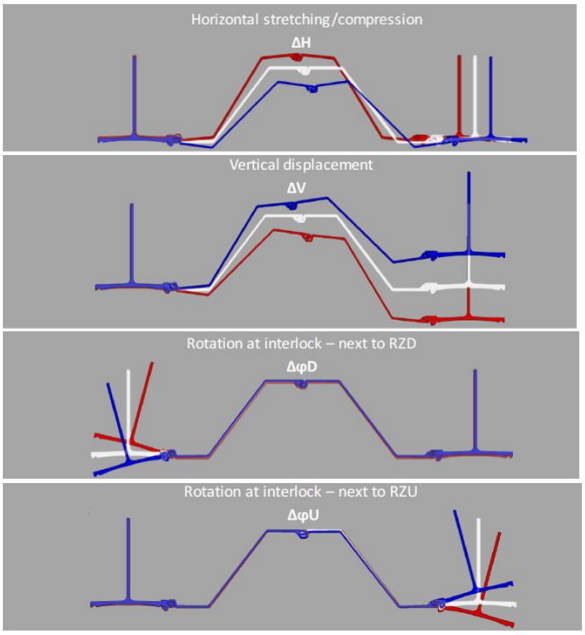

Figure 10. Driving imperfections considered

Following the requirements of prEN 1993-1-14 (CEN, 2021) (Figure 4), two approaches were considered to estimate the resistance of the system.

Since the problem is highly non-linear, with different contacts, the Dynamic Implicit solver was selected for the analysis as it allows an easier convergence. To ensure the required quasi-static behaviour, verification of the energy balance is required, as described in the analysis presented in Section 4.2.

As presented in Section 3.3, the validation of the numerical procedure was performed by applying a pre-

scribed displacement, as considered in the experimental campaign setup (Figure 8). However, the water pressure loading must be simulated as pressure (force) and for this reason, a comparison between a model with prescribed displacement and force was performed.

The use of a model with applied force would not allow the direct identification of the instability point (C1). It can however be identified indirectly by looking at the increase of the kinetic energy of the system. A sensitivity analysis is afterwards presented to identify the best load application speed for the model.

4.2 Stability-based approach

The method proposed for estimating the water pressure resistance of the system corresponding to criterion C1 (Figure 4) is based on the analysis of the kinetic energy of the numerical models, which is a direct output from the software (Abaqus, 2017).

The main premise of this approach is supported by the fact that the maximum allowable/attainable water pressure occurs when the kinetic energy of the model starts to rise in the system.

In the study, a sensitivity analysis on the load application speed was conducted, which allows to show that for decreasing speeds of load application the rise of the kinetic energy becomes very sharp instead of a smooth rise. This allows to identify the exact time step in which the maximum load is reached.

Figure 11 shows the variation of the kinetic energy of different models with different load application speeds from 1 sec (normal) to 10000 sec. The convergence towards a sharp rise can be observed at a load application speed of 100 sec and slower.

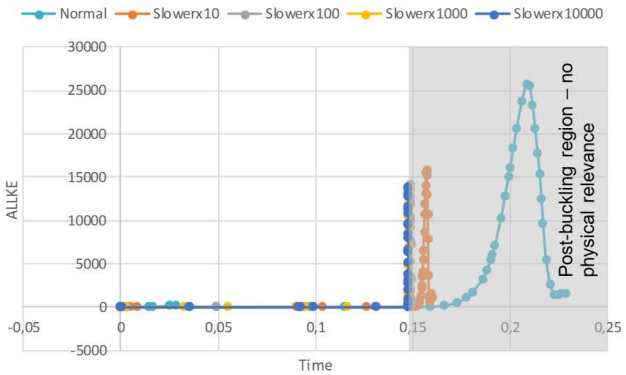

Figure 11. Kinetic energy (ALLKE) variation of models with different load application times – tests in AZ26 Section

To validate this procedure three geometries were evaluated (AZ26, AZ18-800 and AZ14-770) and the output of different types of energies is considered for analysis. In Figure 12, the results for the case of the AZ26 are shown as an example, the comments/trends for the remaining Sections analysed being similar.

In the numerical procedure adopted, the driving imperfections and model stabilization were applied prior to the water pressure loading on steps 1 and 2, respectively (on a numerical time step up to 2 seconds). On Figure 12.a. the water pressure is then applied on the time frame of 2 to 3 seconds while on Figure 12.b. it is applied from 2 to 10002 seconds.

By the analysis of Figure 12, it is possible to observe, for both load application speeds of 1 sec and 10000 sec, that the external work is equal to the internal energy and that the kinetic energy is very small until the rising point, confirming therefore the quasi-static behaviour of the systems until the maximum load is reached.

A comparison between models with prescribed displacement and force has been performed considering the geometry used for the validation procedure and presented in Section 3.3. All models (both with prescribed displacement as with local force) presented the same behaviour up to the point of maximum force, independently of the load application time.

These results show that it is admissible to change from a prescribed displacement simulation (as used to validate the model and generate the results of Section 3.3) to a force-controlled condition to simulate the water pressure as presented in Figure 5.

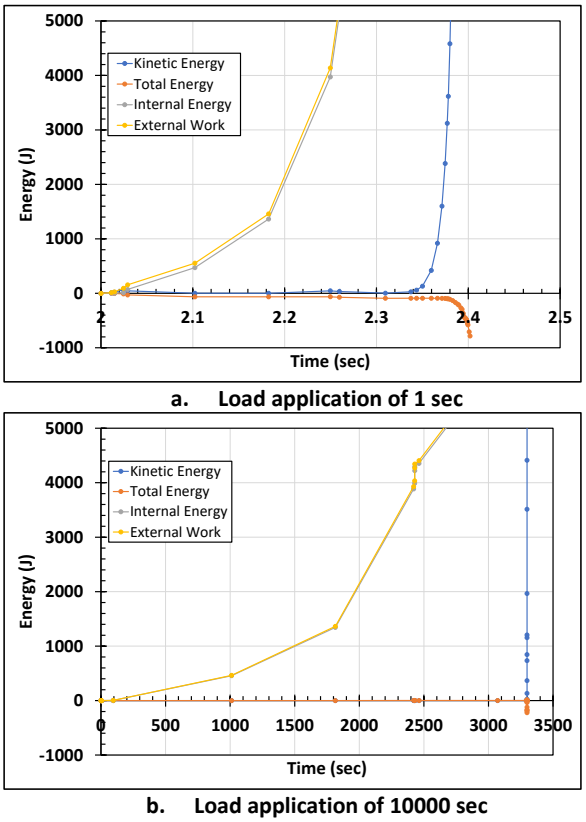

Figure 12. Energy balance for models with different load application times (AZ26 example)

The increase in the kinetic energy of the system occurs at the same time step (water pressure), independently of the loading time (1 or 10000sec). Moreover, it was verified that the rising point of the kinetic energy is coincident with the point of maximum force

obtained in the correspondent force-displacement curves, validating therefore the main premise supporting the numerical technique proposed in the study.

4.3 Strain-based approach

Within the C2 approach (Figure 4), the strain-based method, it is verified the water pressure for which the material of the specimen reached the strain limitation in the mostly stressed fibres.

The default maximum strain in prEN 1993-1-14 (CEN, 2021) is 5%. However, secondary piles need big displacements to achieve equilibrium under water pressure as allowed by EN 1993-5 and thus a higher limit needs to be chosen. Based on the tests performed by Just (2020), the necking strain defined as 60% of the fracture strain according to BSK99 (2003) is considered as acceptable limit.

5 CONCLUSIONS

The HZ®-M wall system is a well implemented retaining system commonly applied in applications requiring high bending resistance. Conditions with high water pressure are frequently found and therefore there is the need to properly assess the performance of these structures under this specific type of loading.

More or less important driving imperfections may occur during installation, depending on the guiding frames used (Kuhlmann et al., 2021). It is important to understand and account for their impact on the water pressure resistance, thus to define tolerances in design, chose an appropriate guiding frame and to remain in the tolerance limits specified for each project.

This study presents a comprehensive description of a numerical modelling technique to estimate the maximum water pressure resistance of an HZ®-M wall (with or without driving imperfections). It allows for for developing a reliable tool to correctly assess the behaviour of the HZ®-M walls under water pressure. It was properly compared and validated with experimental testing results.

This technique covers both possible failure criteria identified in the new generation of Eurocodes (stability (C1) and strain based (C2) criteria).

The stability criteria is based on the analysis of the kinetic energy of the system (the rise of this energy is coincident with the instability point of the system) while the strain-based criteria is based on the measurement of the pressure for which the maximum allowable strain is reached in the model.

6 REFERENCES

Abaqus 2017. *User's manual*, Dassault Systèmes, Simulia Corp.

ArcelorMittal Sheet Piling 2020. *The HZ®-M Steel Wall System*, ArcelorMittal.

BSK99 *2003 Swedish Regulations for Steel Structures. Swedish design code, Handbook*, National Board of Housing Building and Planning, Karlskrona.

CEN 2002. *Eurocode – Basis of structural design*, European Committee for Standardization, Brussels.

CEN 2007. *Eurocode 3 – Design of steel structures – Part 5: Piling*, European Committee for Standardization, Brussels.

CEN 2021. *Eurocode 3: Design of steel structures — Part 1-14: Design assisted by finite element analysis. European Standard (pr EN1993-1-14)*, European Committee for Standardization, Brussels.

CEN 2022. *prEN12063. Execution of special geotechnical work - Sheet-pile walls*, European Committee for Standardization, Brussels.

Chrzanowski, M., Gregor, O., Matos, R., Prüm, C., Zillgen, H., Hechler, O. 2021. Zum Einfluss der Lageimperfektionen auf das Tragverhalten von HZ/AZ-Wänden bei Belastung aus Wasserüberdruck, *Bautechnik* **98**, H. 8, S. 582–594

Just, A. 2020. *Zum Tragverhalten von Stahlspundwänden mit breiten Zwischenbohlen*, PhD Thesis, University of Stuttgart.

Kuhlmann, U., Enders, A., Grabe, J., Beuße, J. 2021. *P 1327 – Optimierte Auslegung von kombinierten Stahlspundwänden für den Einbringvorgang und den Endzustand*, FOSTA report.